High-Efficiency Reconfigurable Dual-Band Class-F Power Amplifier With Harmonic Control Network Using MEMS

Mitra Gilasgar, Antoni Barlabé, *Member, IEEE*, and Lluís Pradell, *Member, IEEE*

***Abstract*— This letter presents a novel reconfigurable, high-efficiency class-F power amplifier (PA) structure, using a commercial GaN-HEMT, that achieves dual-band configuration not only at the fundamental frequency but also at the harmonics. With a proper harmonic tuning structure, the need for an extra filtering section is eliminated, resulting in a high dual-band efficiency with a reduced number of components and size. The reconfigurable structure uses commercial single-pole-double-throw (SPDT) and single-pole-single-throw (SPST) MEMS switches optimally placed on the stubs to select between 900 and 1800 MHz. The reconfigurable PA achieves a measured power-added efficiency (PAE) of 69.5% and a power gain of 13.6 dB while delivering an output power of 39.1 dBm at 900 MHz. At 1800 MHz, the amplifier achieves a PAE of 57.9%, a power gain of 10.5 dB, and an output power of 38.5 dBm.**

***Index Terms*— High efficiency, MEMS, reconfigurable, RF class-F amplifier, RF power amplifier (PA).**

I. Introduction

THE ever-increasing demand for wireless devices for global coverage results in a need for systems to cover multiple frequency bands, capable of serving many users. To achieve the multiband coverage, multiband transceivers and consequently multiband power amplifiers (PAs) are needed.

The PA is a critical block in the transceiver design because it consumes most of the transceiver's dc power. The switching PAs [1], such as class-E/E^{-1} [2] and class-F/F^{-1} [3], can obtain high efficiency. A class-E has a simple load network, but the transistor's large output capacitance decreases the efficiency at high frequencies [4]. This effect is negligible in class-F PAs due to their harmonically tuned output-matching network (OMN) [5], [6].

The conventional multiband operation uses multiple single-frequency PA circuits in one design. This results in a bigger size, a higher cost, and depending on the number of bands that can become impractical. Recent advances for building multiband systems with improved performance and reduced size rely on topologies such as concurrent multiband [7]–[9], broadband [10]–[13], and reconfigurable [14]–[20] circuits. The concurrent multiband circuits achieve matching concurrently in multiple individual bands. This is challenging for class-F amplifiers since they need harmonic tuning as well as fundamental matching, resulting in a very complex circuit design. The broadband circuits compromise performance for bandwidth and, therefore, are not suitable for high-efficiency PA designs. The reconfigurable circuits aim for the high performance associated with narrow-band circuits in multiple single bands and, therefore, exhibit superior behavior compared to the broadband and concurrent circuits. In [19], both reconfiguration and concurrent concepts are used to design a Doherty amplifier. In [20], MEMS are used to switch the amplifier's fundamental frequencies.

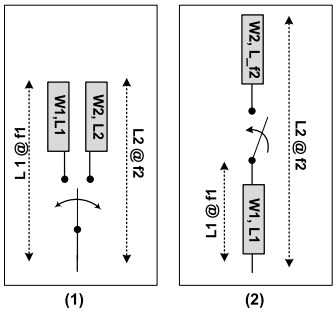

Fig. 1. Implementing the concept for reconfiguration by using (1) SPDT switches and (2) SPST switches.

In this letter, a novel reconfigurable class-F PA using a commercial GaN-HEMT is presented. It switches between two mobile phone frequency bands of 900 MHz and 1.8 GHz using commercial single-pole double-throw (SPDT)/SPST MEMS switches. Switching is performed at the stub level. The proposed structure controls up to the third harmonic independently from the fundamental component. It achieves dual-band configuration at the fundamental and harmonic frequencies, which results in high power-added efficiency (PAE) and very low harmonic distortion. A comparison with previous designs shows that the proposed reconfigurable PA maintains high performance with a reduced number of components and size. This gives a low-cost, dual-band implementation of a high-efficiency class-F PA.

II. Proposed Reconfigurable Class-F PA

A class-F PA uses multiple resonators in its OMN to obtain half-sinusoidal drain current and square drain voltage waveforms. Depending on the application and frequency, the matching network (MN) can be designed with lumped [2] or distributed [6] elements. Implementing lumped-element multiresonators at microwave frequencies becomes complex, while the transmission lines (TLs) offer simpler networks. The

Manuscript received March 11, 2020; revised May 8, 2020; accepted May 10, 2020. This work was supported in part by the Spanish Ministerio de Economía y Competitividad (MEC) under Projects TEC2013-48102-C2-1-P, TEC2016-78028-C3-1-P and Grant BES-2011-051305, in part by the Catalan Agència de Gestió d'Ajuts Universitaris i de Recerca (AGAUR) under Grant 2017-SGR-00219, and in part by the Unidad de Excelencia María de Maeztu through the Agencia Estatal de Investigación (AEI), Spain, under Grant MDM-2016-0600. *(Corresponding author: Lluís Pradell.)*

Mitra Gilasgar was with the Department of Signal Theory and Communications, Universitat Politècnica de Catalunya, 08034 Barcelona, Spain. She is now with Ampleon Netherlands B.V., 6534 AV Nijmegen, The Netherlands (e-mail: mitra.gilasgar@ampleon.com).

Antoni Barlabé and Lluís Pradell are with the Department of Signal Theory and Communications, Universitat Politècnica de Catalunya, 08034 Barcelona, Spain (e-mail: barlabe@tsc.upc.edu; pradell@tsc.upc.edu).

Color versions of one or more of the figures in this letter are available online at http://ieeexplore.ieee.org.

Digital Object Identifier 10.1109/LMWC.2020.2994373

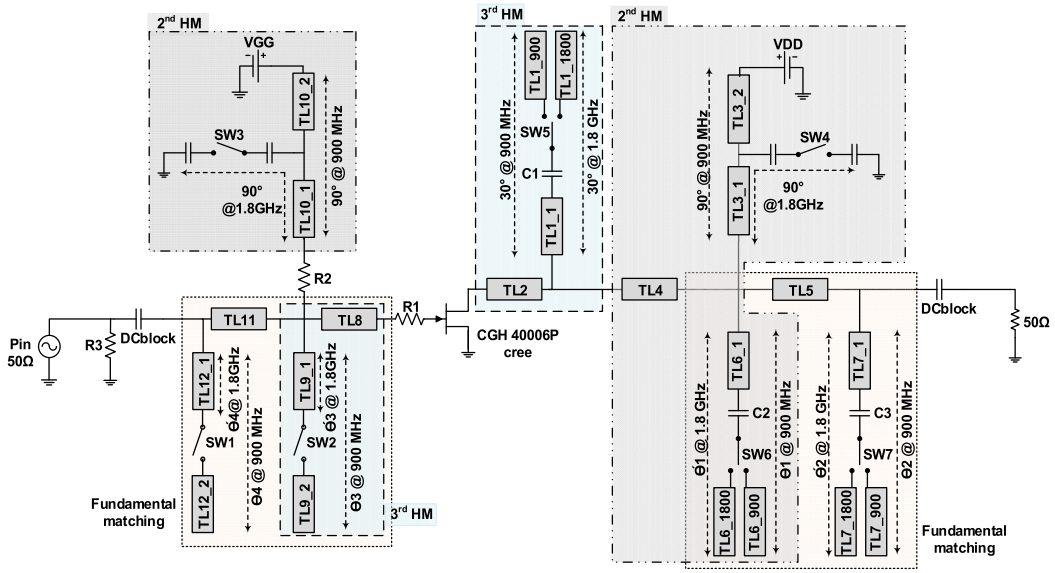

Fig. 2. Proposed reconfigurable class-F PA for the operating frequencies: $f_1 = 900$ MHz and $f_2 = 1800$ MHz. SW1, SW2, and SW4 are RADANT RMSW100HP; SW5, SW6, and SW7 are RADANT RMSW220HP; and SW3 is Hittite HMC550.

periodic behavior of the TL helps to achieve the requirements of a class-F PA at multiple resonant frequencies.

A conventional way to achieve a dual-band class-F PA is to switch between two separate sets of OMN and input MN (IMN), each designed for a certain frequency (f_1 or f_2). This type of reconfiguration is not interesting for TL OMNs because the increased number of frequency bands leads to a big size, higher cost, and complexity of the circuit. The general reconfiguration concept proposed in this letter is shown in Fig. 1. The fundamental and harmonic matching (HM) for each frequency ($n \cdot f_1$, $n \cdot f_2$) is done by the stub-switching using either SPDT or SPST switches. The SPDT switches select between two independent stubs of widths and lengths W1, L1 at f_1 and W2, L2 at f_2, and SPST switches control the length of a single stub from L1 in the OFF-state at f_1 to L1 + L_f2 in the ON-state at f_2.

The proposed reconfigurable dual-band class-F PA is shown in Fig. 2. The PA works at two frequency bands of $f_1 = 900$ MHz and $f_2 = 1800$ MHz. The IMN and OMN each consists of fundamental, second, and third HM blocks. The IMN includes two SPST MEMS switches (SW1 and SW2) and one SPST semiconductor switch (SW3). Since the current and voltage in the gate bias network are low, a semiconductor switch is used here. The OMN includes one SPST MEMS switch (SW4) and three SPDT MEMS switches (SW5, SW6, and SW7). While SPST switches are simpler and cheaper, SPDT switches give more freedom to design for performance and reliability. The OMN is critical for the overall performance and ability to sustain high power; therefore, SPDT switches are used in the OMN. The SPST switches are used in less critical points of the circuit, such as gate bias, drain bias and IMN. The simulations were carried out with Keysight Advanced Design System (ADS) and Momentum software. The models of the transistor (compact nonlinear model) and switches (*S*-parameters models) were supplied by the manufacturers.

A. Input MN

The lengths of the IMN TLs are adjusted using SPST switches. SW1 and SW2 are placed in a cascade between the stubs to provide proper length at each frequency, but SW3 is placed in parallel to assure a proper path for gate biasing.

TABLE I

CALCULATED LOAD IMPEDANCES FOR FUNDAMENTAL, SECOND, AND THIRD HARMONICS OBTAINED FROM LOAD-PULL ANALYSIS

$f_1 = 900$ MHz	Load impedance (Ω)	$f_2 = 1800$ MHz	Load impedance (Ω)
Z_{L1} (@ f_1)	47.7 + j39.1	Z_{L1} (@ f_2)	57.2 + j83.4
Z_{L2} (@ $2f_1$)	2.3 - j13.1	Z_{L2} (@ $2f_2$)	+ j11.9
Z_{L3} (@ $3f_1$)	58.5 + j234.8	Z_{L3} (@ $3f_2$)	- j275.9

The stability of the design has been addressed from an early stage, obtaining unconditional stability, thanks to resistors R_1, R_2, and R_3.

B. Output MN

For an ideal class-F operation, the transistor output should see a short circuit (sc) at the second harmonic, an open circuit (oc) at the third harmonic, and an optimized value at the fundamental frequency. In practice, the second and third harmonic impedance values are determined and optimized using load–pull software techniques [21] and implemented by the networks shown in Fig. 2. The coupling between harmonic networks is minimum, allowing fine independent harmonic load tuning [22]. Table I presents the calculated optimal harmonic load impedances. The same biasing structure as in the IMN is used for the OMN. Using switches in the stubs introduces an extra electrical length which is compensated by adding RF capacitors C_1, C_2, and C_3 in the stub. These capacitors also remove the dc component from the stub, increasing power capability and reliability.

C. Reliability

The high power of a PA brings a challenge to the reliability of the OMN circuit. The pure standing waves on the oc stubs may produce high voltages over the switch in the OFF-state (up to $2 \cdot |V_{ds}|$) and high currents through the switch in the ON-state. In the OFF-state, the voltage drop over the switch should be kept below its breakdown voltage, and the challenge comes from fulfilling this condition in the dual-band operation. RF capacitors C_1, C_2, and C_3, rated at 100 V, are used to modify the electric (and physical) length of the stubs as well as blocking any dc component that could reach the MEMS switches through the RF paths. The resized stub, capacitor

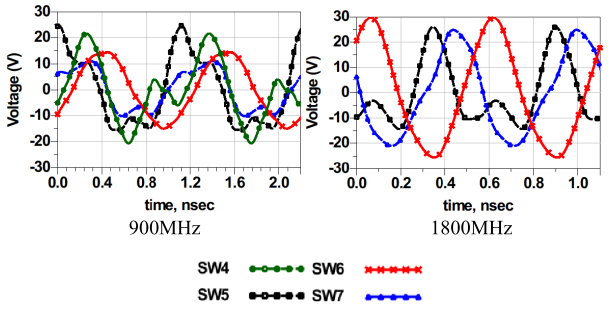

Fig. 3. Simulated RF voltage over the MEMS switches.

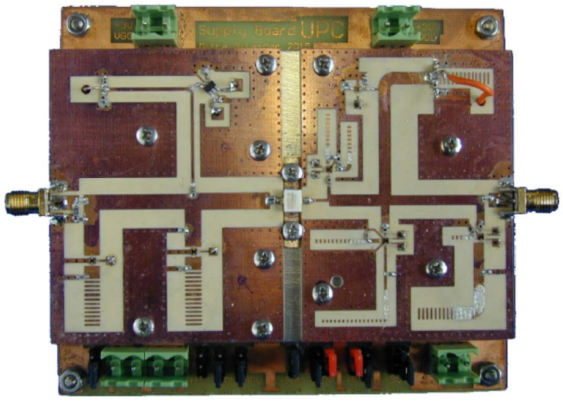

Fig. 4. Fabricated circuit.

value, and their exact placement provide the required reactance for the harmonic filter and allow reliable operation of the MEMS switches. As shown in Fig. 3, the simulations at 900 and 1800 MHz show an RF peak voltage over the OMN MEMS switches of 30 V. The peak voltage over the capacitors is 52 V. Without these capacitors, the voltages can reach unsafe values.

III. Fabrication and Experimental Results

The proposed reconfigurable class-F PA was implemented on a Rogers RO4003 substrate ($h = 1.5$ mm, $\varepsilon_r = 3.55$). The fabricated PA is shown in Fig. 4. The optimal performance is achieved for a drain voltage of 29.5 V and a gate voltage of -1.9 V for the 900-MHz operation and a drain voltage of 33 V and a gate voltage of -2.2 V for the 1800-MHz operation. The performance of the PA was characterized to measure the PAE, drain efficiency (DE), gain, output power (P_{out}), and return loss (RL). The simulation and measurement results versus input power (P_{in}) are shown in Fig. 5, versus frequency in Fig. 6, and versus P_{out} in Fig. 7.

At 900 MHz, the PA features a measured peak PAE of 69.5% and a DE of 72.5% at $P_{\text{in}} = 25.5$ dBm, P_{out} of 39.1 dBm (8.1 W), and a gain of 13.8 dB. At 1800 MHz, the PA delivers a measured P_{out} of 38.5 dBm (7.1 W) at $P_{\text{in}} = 28$ dBm where it achieves a maximum PAE of 57.9% and a DE of 63.5%. The gain is 10.5 dB. The RL is better than 10 dB at both operating frequencies for input powers up to 25 dBm. Fig. 6 shows that the PA exhibits a 10% bandwidth for PAE and DE and a much wider bandwidth for P_{out} and gain. Fig. 7 shows a good agreement between the simulated and measured results of PAE and DE. The total harmonic distortion (THD) is 6.5% for the 900-MHz operation and 4.1% for the 1800-MHz operation. These results confirm that the proposed topology has the ability to reject harmonics without the need for an extra filtering section.

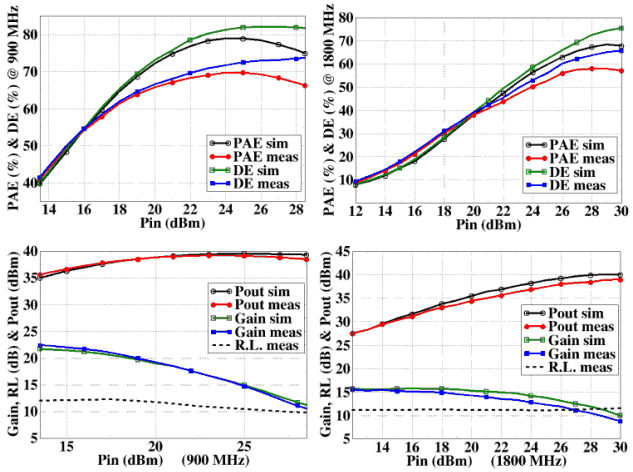

Fig. 5. Measured and simulated PAE, DE, gain, P_{out}, and RL versus P_{in}.

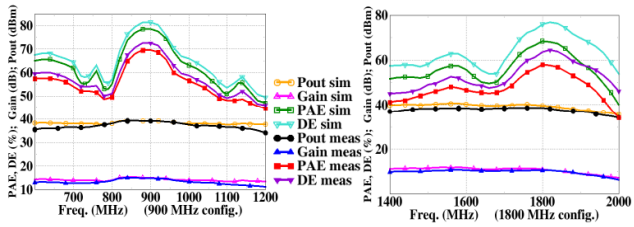

Fig. 6. Measured and simulated P_{out}, gain, PAE, and DE versus frequency.

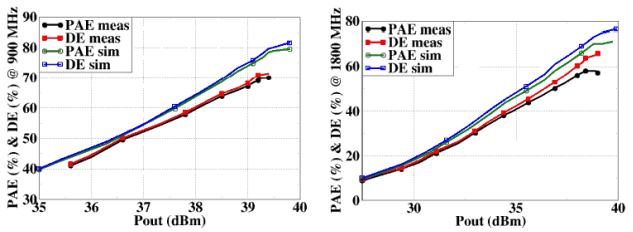

Fig. 7. Measured and simulated PAE, and DE versus P_{out}.

TABLE II
Comparison of This Work With Other Works

	Tech.	Freq. (GHz)	PAE (%)	DE (%)	Gain (dB)	Pout (dBm)
[7]	GaAs	1.7/ 2.14	31/ 50	44 / 61.3	5 / 4.5	32.8 / 34.4
[10]	GaN	1.5/ 2.5	58 / 60	61 / 73.5	9.5	39.5
[13]	GaN	2.4/ 3.9	57.5 / 69.1	62.2 /74.7	10.7 /12.5	39.6 / 41.4
[18]	GaN	0.9/ 1.45	-	60 / 76	>9.6	-
This	**GaN**	**0.9 / 1.8**	**69.5 / 57.9**	**72.5 /63.5**	**13.6 /10.5**	**39.1 / 38.5**

A comparison of our design with other dual-band PAs in the literature shown in Table II shows that the proposed structure achieves a PAE and a DE higher than the other references while providing high P_{out} and gain.

IV. Conclusion

This letter presents a novel frequency-reconfigurable class-F PA based on a stub-switching concept using commercial SPDT and SPST MEMS switches in the MNs. It is suitable for any passband signal centered at 900 or 1800 MHz. The proposed structure controls the fundamental matching independently from the harmonics, achieving excellent performance. They also provide high harmonic rejection without the need for extra filtering sections. The measurement results showed a peak PAE of 69.5% and 57.9% and P_{out} of 8.1 and 7.1 W for the operating frequencies of 900 and 1800 MHz, respectively.

REFERENCES

[1] S. C. Cripps, *RF Power Amplifiers for Wireless Communications*. Norwood, MA, USA: Artech House, 1999.

[2] R. Negra and W. Bachtold, "Lumped-element load-network design for class-E power amplifiers," *IEEE Trans. Microw. Theory Techn.*, vol. 54, no. 6, pp. 2684–2690, Jun. 2006.

[3] F. H. Raab, "Class-F power amplifiers with maximally flat waveforms," *IEEE Trans. Microw. Theory Techn.*, vol. 45, no. 11, pp. 2007–2012, Nov. 1997.

[4] A. Mediano, P. Molina-Gaudo, and C. Bernal, "Design of class E amplifier with nonlinear and linear shunt capacitances for any duty cycle," *IEEE Trans. Microw. Theory Techn.*, vol. 55, no. 3, pp. 484–492, Mar. 2007.

[5] J. Moon, S. Jee, J. Kim, J. Kim, and B. Kim, "Behaviors of class-F and class-F^{-1} amplifiers," *IEEE Trans. Microw. Theory Tech*, vol. 60, no. 6, pp. 1937–1951, Jun. 2012.

[6] R. Negra, F. M. Ghannouchi, and W. Bachtold, "Study and design optimization of multiharmonic transmission-line load networks for class-E and class-F K-band MMIC power amplifiers," *IEEE Trans. Microw. Theory Techn.*, vol. 55, no. 6, pp. 1390–1397, Jun. 2007.

[7] R. Negra, A. Sadeve, S. Bensmida, and F. M. Ghannouchi, "Concurrent dual-band class-F load coupling network for applications at 1.7 and 2.14 GHz," *IEEE Trans. Circuits Syst. II, Exp. Briefs*, vol. 55, no. 3, pp. 259–263, Mar. 2008.

[8] Q.-F. Cheng, H.-P. Fu, S.-K. Zhu, and J.-G. Ma, "Two-stage high-efficiency concurrent dual-band harmonic-tuned power amplifier," *IEEE Trans. Microw. Theory Techn.*, vol. 64, no. 10, pp. 3232–3243, Oct. 2016.

[9] J. Li, W. Chen, F. Huang, and Z. Feng, "Multiband and multimode concurrent PA with novel intermodulation tuning network for linearity improvement," *IEEE Microw. Wireless Compon. Lett.*, vol. 28, no. 3, pp. 248–250, Mar. 2018.

[10] E. Aggrawal, K. Rawat, and P. Roblin, "Investigating continuous class-F power amplifier using nonlinear embedding model," *IEEE Microw. Wireless Compon. Lett.*, vol. 27, no. 6, pp. 593–595, Jun. 2017.

[11] H. Huang, B. Zhang, C. Yu, J. Gao, Y. Wu, and Y. Liu, "Design of multioctave bandwidth power amplifier based on resistive second-harmonic impedance continuous class-F," *IEEE Microw. Wireless Compon. Lett.*, vol. 27, no. 9, pp. 830–832, Sep. 2017.

[12] Y. Sun and X. Zhu, "Broadband continuous class-F^{-1} amplifier with modified harmonic-controlled network for advanced long term evolution application," *IEEE Microw. Wireless Compon. Lett.*, vol. 25, no. 4, pp. 250–252, Apr. 2015.

[13] W. Shi, S. He, and Q. Li, "A series of inverse continuous modes for designing broadband power amplifiers," *IEEE Microw. Wireless Compon. Lett.*, vol. 26, no. 7, pp. 525–527, Jul. 2016.

[14] A. M. M. Mohamed, S. Boumaiza, and R. R. Mansour, "Novel reconfigurable fundamental/harmonic matching network for enhancing the efficiency of power amplifiers," in *Proc. 40th Eur. Microw. Conf.*, Paris, France, Sep. 2010, pp. 1122–1125.

[15] A. M. Mahmoud Mohamed, S. Boumaiza, and R. R. Mansour, "Reconfigurable Doherty power amplifier for multifrequency wireless radio systems," *IEEE Trans. Microw. Theory Techn.*, vol. 61, no. 4, pp. 1588–1598, Apr. 2013.

[16] M. Gilasgar, A. Barlabe, and L. Pradell, "A 2.4 GHz CMOS class-F power amplifier with reconfigurable load-impedance matching," *IEEE Trans. Circuits Syst. I, Reg. Papers*, vol. 66, no. 1, pp. 31–42, Jan. 2019.

[17] K. K. Sessou and N. M. Neihart, "An integrated 700–1200-MHz class-F PA with tunable harmonic terminations in 0.13-μm CMOS," *IEEE Trans. Microw. Theory Techn.*, vol. 63, no. 4, pp. 1315–1323, Apr. 2015.

[18] K. Han, Y. Yang, C. J. You, X. Zhu, and X. Du, "Reconfigurable continuous class-F power amplifier using tunable output matching network," in *Proc. IEEE 17th Int. Conf. Commun. Technol. (ICCT)*, Oct. 2017, pp. 1201–1204.

[19] R. Kalyan, K. Rawat, and S. K. Koul, "Reconfigurable and concurrent dual-band Doherty power amplifier for multiband and multistandard applications," *IEEE Trans. Microw. Theory Techn.*, vol. 65, no. 1, pp. 198–208, Jan. 2017.

[20] R. Malmqvist *et al.*, "RF MEMS and MMIC based reconfigurable matching networks for adaptive multi-band RF front-ends," in *Proc. IEEE Int. Microw. Workshop RF Front-Ends Softw. Defined Cognit. Radio Solutions (IMWS)*, Aveiro, Portugal, Feb. 2010, pp. 1–4.

[21] Q. Cai, J. Gerber, and S. Peng, "A systematic scheme for power amplifier design using a multi-harmonic loadpull simulation technique," in *IEEE MTT-S Int. Microw. Symp. Dig.*, Baltimore, MD, USA, vol. 1, Jun. 1998, pp. 161–165.

[22] M. Gilasgar, A. Barlabé, and L. Pradell, "Highly efficient class-F RF power amplifiers with very low distortion," *URSI Radio Sci. Bull.*, no. 347, pp. 21–31, 2013.